nature photonics

LETTERS

PUBLISHED ONLINE: 10 JANUARY 2012 | DOI: 10.1038/NPHOTON.2011.318

Extremely efficient flexible organic light-emitting diodes with modified graphene anode

Tae-Hee Han[1], Youngbin Lee[2], Mi-Ri Choi[1], Seong-Hoon Woo[1], Sang-Hoon Bae[2], Byung Hee Hong[3], Jong-Hyun Ahn[2]* and Tae-Woo Lee[1]*

Although graphene films have a strong potential to replace indium tin oxide anodes in organic light-emitting diodes (OLEDs), to date, the luminous efficiency of OLEDs with graphene anodes has been limited by a lack of efficient methods to improve the low work function and reduce the sheet resistance of graphene films to the levels required for electrodes[1–4]. Here, we fabricate flexible OLEDs by modifying the graphene anode to have a high work function and low sheet resistance, and thus achieve extremely high luminous efficiencies (37.2 lm W^{-1} in fluorescent OLEDs, 102.7 lm W^{-1} in phosphorescent OLEDs), which are significantly higher than those of optimized devices with an indium tin oxide anode (24.1 lm W^{-1} in fluorescent OLEDs, 85.6 lm W^{-1} in phosphorescent OLEDs). We also fabricate flexible white OLED lighting devices using the graphene anode. These results demonstrate the great potential of graphene anodes for use in a wide variety of high-performance flexible organic optoelectronics.

Graphene is a flexible two-dimensional sheet of sp^2-hybridized carbon atoms[5–12] that has potential applications in a variety of electronic devices[1–4,13–19]. Finding a way to replace the conventional brittle indium tin oxide (ITO) electrode with a flexible graphene electrode is a major research topic[20]. ITO has been used widely in optoelectronic devices such as organic light-emitting diodes (OLEDs) and liquid-crystal displays, but its raw materials are becoming increasingly expensive, and it is brittle, rendering it unsuitable for flexible devices[20]. It is therefore desirable to develop alternative transparent and flexible electrodes such as graphene.

Despite its strong potential as a transparent conductor, the practical application of graphene as the anode of organic optoelectronic devices has been limited because of its relatively low work function (WF) (~4.4 eV, Supplementary Table S2) and high sheet resistance (>300 $\Omega\,\square^{-1}$ in refs 3,4) compared with ITO (~4.7 ≤ WF ≤ 4.9 eV and 10 $\Omega\,\square^{-1}$). The low WF of graphene causes the hole injection between the graphene anode and the overlying organic layers to be unfavourable because of the high injection barrier at the interface (Fig. 1a) (for example, the ionization potential of *N*,*N*′-bis(naphthalen-1-yl)-*N*,*N*′-bis(phenyl) benzidine (NPB) is ~5.4 eV). As a result, graphene-based OLEDs have shown poorer current efficiencies (CEs, units cd A^{-1}) than ITO-based devices[3,4] (Supplementary Table S3, Fig. S3). In addition, the low conductivity of pristine graphene films limits the luminous (power) efficiencies (LEs, units lm W^{-1}) of the devices because it gives rise to high operating voltages. To achieve practical graphene anodes, a method to eliminate these disadvantages of graphene (low WF and high sheet resistance) needs to be developed.

Here, we demonstrate a method to increase the surface WF and reduce the sheet resistance of graphene films to ~5.95 eV and ~30 $\Omega\,\square^{-1}$, respectively, by using conducting polymer compositions to modify the surface, thus creating a WF gradient from the graphene to the overlying organic layer, and by doping with p-dopants HNO_3 or $AuCl_3$ (Supplementary Tables S4,S5). The higher WF enables holes to be injected easily into the organic layer despite the high hole-injection barrier at the interface between the graphene anode and the organic layer.

We used WF-tunable polymeric conducting polymers to improve hole injection from the anode to the organic layer. Without a hole-injection layer (HIL), hole injection from the graphene anode to the overlying hole-transport layer (HTL; for example, NPB) is unfavourable because of the huge hole-injection energy barrier (~1.0 eV) at the interface (Fig. 1a). To achieve a high CE in OLEDs that have graphene anodes, the efficiency of hole injection from the graphene electrode to the overlying organic layers must be increased. To meet this requirement, we incorporated a self-organized gradient HIL (which we term 'GraHIL') composed of poly(3,4-ethylenedioxythiophene) doped with poly(styrenesulphonate) (PEDOT:PSS) and a tetrafluoroethylene-perfluoro-3,6-dioxa-4-methyl-7-octenesulphonic acid copolymer, one of the perfluorinated ionomers (PFI; Supplementary Fig. S6), which provides a WF gradient through the layer (surface WF = 5.95 eV; Fig. 1b) and thus enables holes to be injected efficiently to the overlying organic layer (ref. 21; Supplementary Table S4, Fig. S7).

To use graphene films as electrodes in flexible electronics, large-area synthesis and an efficient transfer method are essential[1–4,8,18]. Large-scale synthesis of graphene films can be achieved using chemical vapour deposition (CVD)[8–12]. To form a graphene anode on a flexible poly(ethyleneterephthalate) (PET) substrate (Fig. 1e), multilayered graphene films were transferred to a PET substrate using a poly(methyl methacrylate) (PMMA) polymer support or a thermal release tape. The transferred multilayered graphene films were then etched using a pre-patterned shadow mask and reactive ion etching with O_2 plasma. We used our polymeric HILs (GraHIL) to modify the patterned graphene anode.

We fabricated a series of small-molecule fluorescent OLEDs, including a control device with an ITO anode and several experimental devices with multilayered graphene anodes (two, three or four graphene layers). The graphene films were p-doped with HNO_3 or $AuCl_3$ to decrease their sheet resistance.

We measured the CEs and LEs of the devices fabricated using different kinds of HILs. For the ITO-based devices with our self-organized polymeric HILs, GraHIL, the CE was ~18.4 cd A^{-1} (LE ≈ 24.1 lm W^{-1}), which was much higher than that of the device with a conventional small-molecule hole-injection material,

[1]Department of Materials Science and Engineering, Pohang University of Science and Technology (POSTECH), Pohang, Gyungbuk 790-784, Republic of Korea, [2]SKKU Advanced Institute of Nanotechnology (SAINT), Center for Human Interface Nano Technology (HINT) and School of Advanced Materials Science and Engineering, Sungkyunkwan University, Suwon, Gyeonggi-do 440-746, Republic of Korea, [3]Department of Chemistry, Seoul National University, Seoul 151-747, Republic of Korea. *e-mail: twlee@postech.ac.kr; ahnj@skku.edu

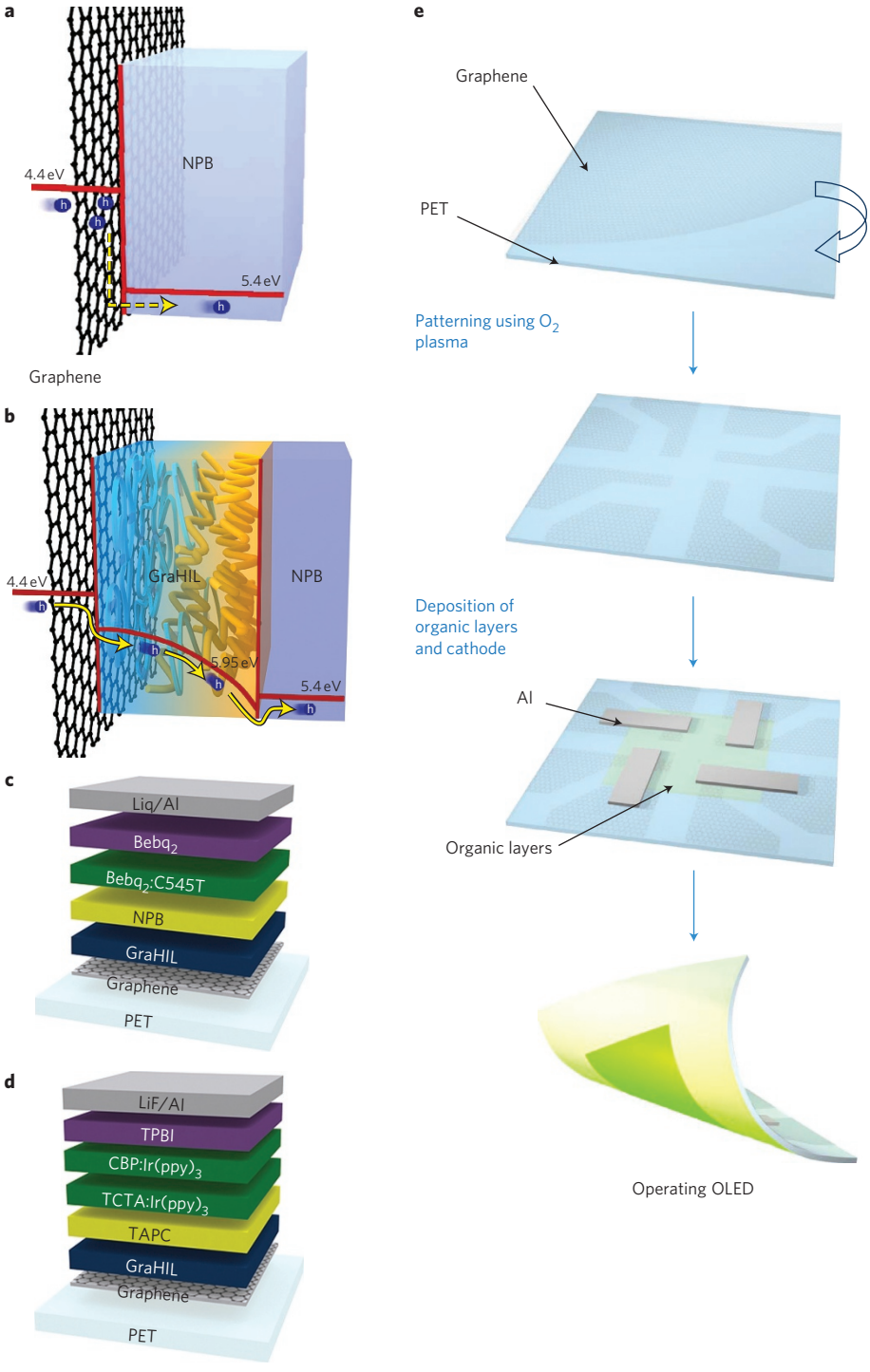

Figure 1 | Schematic illustrations of hole injection from graphene, device structure and fabrication steps for flexible OLEDs. a, Schematic illustration of a hole-injection process from a graphene anode to a conventional HTL (NPB) used in OLEDs. **b**, Schematic illustration of a hole-injection process from a graphene anode via a self-organized HIL with work-function gradient (GraHIL) to the NPB layer. **c**,**d**, Device structures of flexible small-molecule fluorescent OLEDs (**c**) and phosphorescent OLEDs (**d**) using a graphene anode modified with a GraHIL. **e**, Schematic illustration of fabrication steps for flexible OLEDs with a graphene anode.

4,4′,4″-tris(*n*-(2-naphthyl)-*n*-phenyl-amino)-triphenylamine (2TNATA) (CE ≈ 13.7 cd A^{-1}, LE ≈ 16.1 lm W^{-1}) (Fig. 2a,c). This increase in CE and LE can be attributed to the combination of efficient hole injection and electron blocking by the self-organized PFI surface layer, which increases the rate of electron–hole recombination.

When we fabricated green fluorescent OLED devices with anodes consisting of two, three or four layers of graphene doped with HNO_3, the luminance, CE and LE tended to increase due to the increased WF values and reduced sheet resistance as the number of graphene layers increases (Fig. 2a–c) (Supplementary Table S2,S5), even if the reduced optical transparency of multilayer graphenes can have a negative effect on the device efficiencies (CE and LE). This implies that the sheet resistance and the WF were dominant effects on the CE and LE. When the four-layer graphene

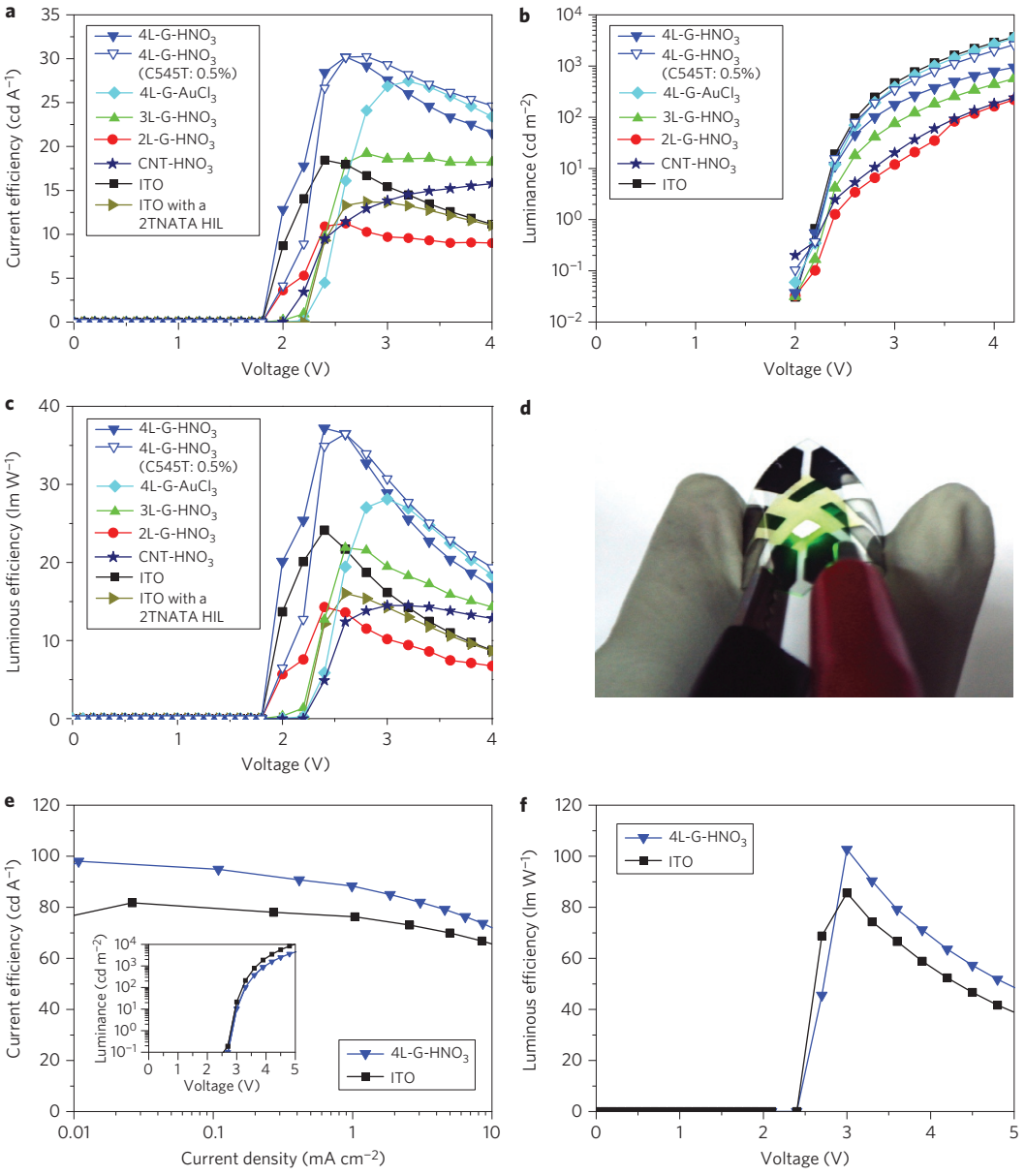

Figure 2 | Performance of green OLEDs with graphene, carbon nanotube and ITO anodes. a–c, Current efficiencies (**a**), luminance (**b**) and luminous (power) efficiencies (**c**) of OLED devices using various graphene layers (doped with HNO_3 or $AuCl_3$) or ITO as anode. **d**, Optical image of light emission from a flexible fluorescent green OLED with a four-layered graphene anode (4L-G) doped with HNO_3 (4L-G-HNO_3). **e**, Current efficiencies of phosphorescent OLED devices using 4L-G-HNO_3 and ITO anodes, as a function of current density. Inset: luminance as a function of voltage in the OLEDs. **f**, Luminous efficiencies of phosphorescent OLED devices. All devices include GraHIL except for ITO (2TNATA).

anode was doped using $AuCl_3$ instead of HNO_3 to decrease the graphene sheet resistance (~30 $\Omega\square^{-1}$), the luminance versus voltage characteristics of the device were nearly identical to those of the device with the ITO anode (Fig. 2b). This similarity implies that the operating voltage is governed by the sheet resistance of the graphene anode.

Devices with four-layer graphene anodes doped with HNO_3 or $AuCl_3$ showed extremely high maximum CEs of 30.2 cd A^{-1} (LE ≈ 37.2 lm W^{-1}) and 27.4 cd A^{-1} (LE ≈ 28.1 lm W^{-1}), respectively (Fig. 2a,c), values that are significantly higher than for devices with an ITO anode including our GraHIL. The efficiency roll-off as a function of voltage was reduced by optimizing the 10-(2-benzothiazolyl) - 1,1,7,7 - tetramethyl - 2,3,6,7 - tetrahydro - 1H,5H,11H-[l]benzopyrano[6,7,8-ij]quinolizin-11-one (C545T) doping concentration from ~1.5% to ~0.5%, as shown in Fig. 2a,c. Although the graphene doped with $AuCl_3$ provides lower sheet resistance and WF values (Supplementary Tables S2,S5), the CE was slightly lower than for devices doped with HNO_3. This is attributed to the formation of gold clusters on top of the surface of the graphene anode during reduction to the gold atoms, giving rise to a local thinning effect causing an increase in leakage current in the devices (Supplementary Fig. S8). The achieved device efficiencies (CE and LE) are more than twice that of the conventional standard device that has a conventional small-molecule hole-injecting material, 2TNATA, on top of the ITO anode (13.7 cd A^{-1}, 16.1 lm W^{-1}). The device with a carbon nanotube (CNT) anode (surface resistivity, ~373.7 $\Omega\square^{-1}$; thickness, ~60 nm; for transmittance see Supplementary Fig. S1) exhibited a poorer maximum CE of 15.8 cd A^{-1} and LE of 14.5 lm W^{-1} (Fig. 2a,c) than those of graphene anode-based devices, which is attributed to limited conductivity and

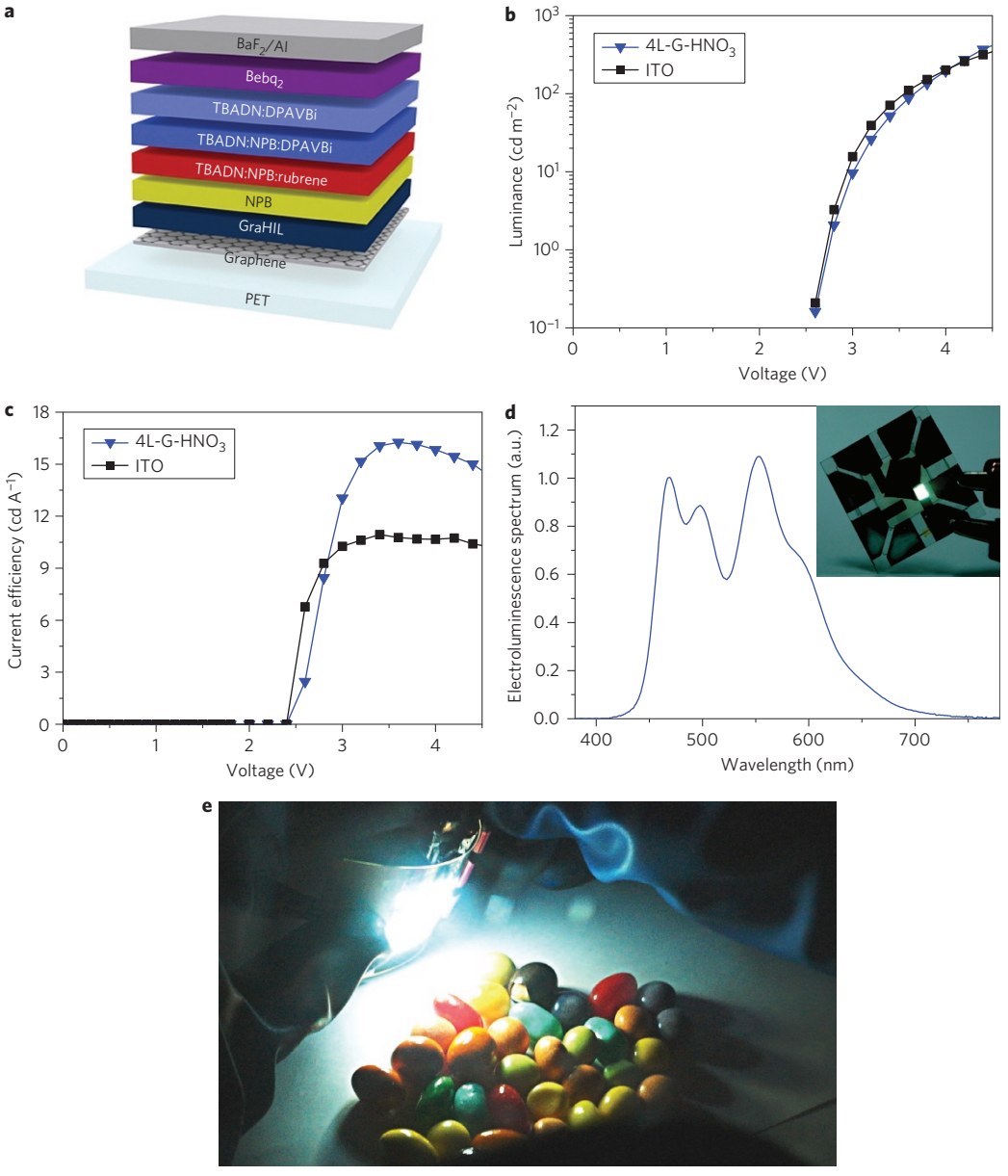

Figure 3 | Device structure and performance of white OLEDs with a graphene anode, and the flexible OLED lighting device. a–c, Device structure (**a**), luminance (**b**) and current efficiency (**c**) as a function of voltage for flexible white OLED devices with graphene (doped with HNO_3) and ITO anodes. **d**, Electroluminescence spectrum of flexible white OLEDs with the four-layered graphene anode and an optical image of white light emission from the device (inset). **e**, Flexible OLED lighting device with a graphene anode on a 5 cm × 5 cm PET substrate.

transmittance. Also, the surface roughness of the anodes can lead to electrical shorts and leakage current in the resulting devices, and it was found that CNT films on PET substrates have a much rougher surface than four-layered graphene film (root-mean-square roughness of CNT, ~15.9 nm) (Supplementary Figs S4,S5). In summary, these results, which show the superiority of graphene anodes over common transparent electrodes such as those based on ITO and CNTs (Supplementary Table S3, Fig. S3), demonstrate the great potential of graphene anodes for applications in organic optoelectronics as well as the importance of overcoming the high hole-injection barrier by molecularly modifying the graphene. It also suggests that previous carbon-based anodes had lower CE values than ITO anodes mainly because of a failure to overcome the huge hole-injection barriers[3,4,22,23].

Because our devices are highly flexible (Fig. 2d), we performed a bending test on the fluorescent green OLED device with a four-layered graphene anode and ITO. The bending radius was found to be 0.75 cm and the strain estimated as 1.25%. We found that the graphene device maintained almost the same current density even after 1,000 bending events, whereas the ITO device failed completely after 800 events (Supplementary Fig. S9). In other words, the graphene anode demonstrated excellent bending stability.

We also fabricated highly efficient flexible phosphorescent green OLEDs using an HNO_3-doped four-layered graphene anode, in which the emitting dopant was tris(2-phenylpyridine)iridium(III) ($Ir(ppy)_3$) (Fig. 1d). The device showed much higher device efficiencies (CE ≈ 98.1 cd A^{-1}, LE ≈ 102.7 lm W^{-1}) than those of the device with an ITO anode (81.8 cd A^{-1} and 85.60 lm W^{-1}) (Fig. 2e,f). The remarkable maximum CE we achieved (98.1 cd A^{-1}) in the flexible OLED devices slightly outperformed the CE value of state-of-the-art non-flexible phosphorescent OLEDs without an outcoupling structure (~93.8 cd A^{-1})[24].

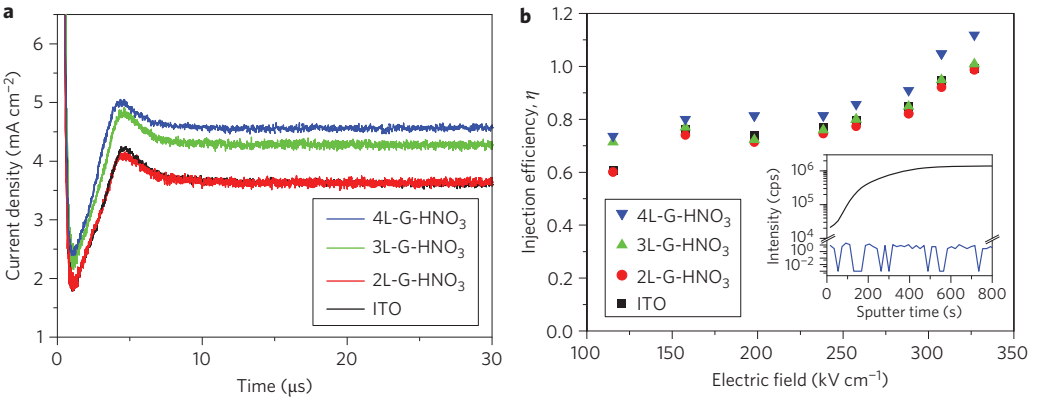

Figure 4 | DI SCLC transient current and hole-injection efficiency of graphene anodes and ITO anode. a, DI SCLC transient currents measured at 30 V in the hole-only devices with anode (graphene or ITO)/GraHIL/NPB (2.6 μm). **b,** Hole-injection efficiencies η obtained by DI SCLC measurements. Inset: depth profile of indium atoms from the surface to the bottom of the GraHIL film for the four-layered graphene (blue line) and ITO substrate (black line).

We also fabricated efficient fluorescent white OLEDs using a four-layered graphene anode doped with HNO_3 (Fig. 3a), in which emitting dopants using two complementary colours (sky-blue-emitting 4,4′-bis[2-{4-(*N*,*N*-diphenylamino)phenyl}vinyl] (DPAVBi) and orange-red-emitting 5,6,11,12-tetraphenylnaphthacene (rubrene)) were doped into separate layers using 2-(tert-butyl)-9,10-bis(2′-naphthyl)anthracene (TBADN) as their host material. The white OLEDs using graphene anodes had operating voltages similar to that using an ITO anode (Fig. 3b). Furthermore, the white device with the graphene anode exhibited a much higher CE (16.3 cd A^{-1}) than that with the ITO anode (10.9 cd A^{-1}) (Fig. 3c) and good white electroluminescence spectra with a Commission Internationale de l'Eclairage (CIE) coordinate (0.32, 0.42) (Fig. 3d). We finally fabricated a flexible white OLED lighting device on a 5×5 cm^2 PET substrate (Fig. 3e). These results demonstrate the promising application of graphene anodes in future flexible solid-state lighting devices.

The optical outcoupling efficiencies of OLED devices with both graphene and ITO anodes were nearly the same according to optical simulation[3]. To understand the cause of the remarkable improvement in CEs obtained using a graphene/GraHIL hole-injection contact, we performed dark-injection space-charge-limited-current (DI SCLC) transient measurements. The DI SCLC transient of hole-only devices with (graphene or ITO)/GraHIL/NPB (~2.6 μm)/aluminium at 30 V (Fig. 4a), had a shape typical of the DI SCLC transient, implying that ohmic contacts had formed between the anodes/GraHIL and the NPB layer in all of the devices[25–28].

We calculated the hole injection efficiency η of each device (see Supplementary Information)[25,28]. Values of η tended to increase with the number of graphene layers. The anode with four graphene layers had a higher hole-injection efficiency than the ITO anode (Fig. 4a,b). Similarly, the calculated hole-injection efficiency as a function of electric field was greatest in graphene anodes with four layers and showed nearly ohmic contact ($\eta \approx 1$). These results indicate that graphene anodes can be used to make OLED devices and that have a more favourable hole-injecting interface between the anode and organic layer (NPB) than with an ITO anode.

The improvement in hole-injection efficiency (value of η) in using graphene, and thus the feasibility of using graphene anodes, now enables us to avoid a serious drawback of using ITO in anodes. ITO releases indium and tin atoms during spin-coating of acidic conjugated polymer dispersions, and these atoms can diffuse into the overlying organic layers[21,29]. The depth profile of indium atoms from the surface to the bottom of the GraHIL films on the ITO and four-layered graphene substrate, obtained using dynamic secondary ion mass spectroscopy (SIMS), clearly demonstrates that a substantial proportion of the diffused indium atoms lies between the ITO anode and the surface of the HIL film, but no diffused indium atoms are found in the HIL film on the graphene anode (Fig. 4b, inset) These atoms can form interfacial trap states that trap holes at the interface between the anode and the organic layers. These traps reduce the hole-injection efficiency of the ITO. We did not observe a rapidly decaying current transient starting from the peak in the DI SCLC transient curves, so the interfacial traps are fast traps rather than slow traps[28]. From our results, we conclude that graphene anodes are nearly trap-free, and form excellent hole-injection interfaces with organic layers.

In conclusion, we have achieved extremely high maximum CEs (30.2 cd A^{-1} and 98.1 cd A^{-1}) and LEs (37.2 lm W^{-1} and 102.7 lm W^{-1}) in flexible fluorescent and phosphorescent OLEDs with four-layered graphenes by modifying the surface with our conducting polymer, which has a gradient work function. These remarkable device efficiencies increase the feasibility of using graphene anodes to make extremely high-performance flexible organic optoelectronic devices by overcoming the major drawbacks (low work function and trap formation due to diffusion of indium and tin) of conventional ITO anodes. This approach demonstrates a way to increase device performance greatly by replacing ITO anodes with flexible graphene anodes in organic optoelectronic devices such as flexible, stretchable full-colour displays[30] and solid-state lighting.

Methods

Graphene growth and fabrication of patterned graphene anodes. Copper foils in the inner quartz tubes were inserted into a tubular quartz tube of a CVD system before the growth process. The foils were then heated to 1,000 °C with 10 s.c.c.m. flow of H_2 gas under 80 mtorr of pressure for 30 min. In the same flow of H_2 gas and pressure, the copper foils were annealed at 1,000 °C for 30 min. In the growth step, the precursor gas CH_4 (15 s.c.c.m.) was injected at a pressure of ~1.6 torr for 30 min. After this step, the copper foils were rapidly cooled to room temperature. This thermal CVD process based on copper catalytic material resulted in a graphene film with a uniform monolayer coverage of >95% with high quality.

To form the multilayered graphene film using graphene films on copper foils, a coating of PMMA or thermal release tape (TRT) was applied onto the graphene/copper foil as the first step of the transfer process. After etching of the copper foil, we delivered the polymer/graphene film onto the other graphene/copper foil instead of a target substrate, because the repetition of this process resulted in the formation of multilayered graphene without an additional polymer-coating process. One of the advantages of this procedure is avoiding any residual polymer residues between each layer in the final multilayered graphene. When the desired number of stacks was achieved, it was transferred onto the target substrate (in this work, PET). The PMMA support was effectively removed using acetone boiled up to 80 °C. The TRT support was detached by removing the adhesive force holding the graphene using a 90 °C thermal treatment performed with a roll-to-roll laminator.

To form the graphene anode pattern without organic residue, we used a shadow mask and oxygen plasma etching (70 mtorr, 100 W, 3 s) instead of a photolithography process. If a microscale pattern were required, a photolithography procedure could be added to this procedure. The graphene films were p-doped with HNO_3 or $AuCl_3$ to increase their conductivity (changes of sheet resistance with time is shown in Supplementary Fig. S10).

Although the conductivities of the present graphene films made using the CVD method are moderate, it might be possible to further improve the electrical properties by developing a growth mechanism for large grains with a well-connected grain boundary and a method to transfer a very flat, defect-free graphene film to a substrate without generating ripples and cracks, which in turn would lead to further improvement of the organic device performance.

OLED fabrication. A patterned graphene anode, a CNT-based anode (TOP NANOSYS: thickness, ~60 nm; sheet resistance, ~373.7 $\Omega\square^{-1}$) on a PET substrate (Fig. 1e) and an ITO anode ($\sim 4.7 \leq WF \leq 4.9$ eV, 10 $\Omega\square^{-1}$) on a glass substrate were UV-ozone treated for 10 min. The polymeric hole-injection layer (GraHIL), composed of PEDOT:PSS (CLEVIOS P VP AI4083) and a PFI (tetrafluoroethylene-perfluoro-3,6-dioxa-4-methyl-7-octenesulphonic acid copolymer, CAS number 31175-20-9, Sigma-Aldrich) in a 1:1 ratio, was spin-coated to give a 50-nm-thick film on top of the anodes and then baked immediately on a hot plate in air at 150 °C for 30 min. For comparison, we deposited a small-molecule HIL, 2TNATA, as the HIL under high vacuum. Organic layers consisting of 20-nm-thick NPB as the HTL, 30-nm-thick bis(10-hydroxybenzo[h]quinolinato)beryllium ($Bebq_2$) doped with (C545T, ~1.5%), and 20-nm-thick $Bebq_2$ were sequentially deposited on the HILs under high vacuum. Cathode layers of 8-hydroxyquinoline lithium (Liq) (1 nm)/aluminium (130 nm) were deposited under high vacuum.

For the fabrication of phosphorescent green OLEDs, a 50-nm-thick GraHIL was spin-coated on the graphene anode. The green-emitting dopant material, tris(2-phenylpyridine)iridium(III) ($Ir(ppy)_3$), was doped into two different layers (5 nm for each) with 1,1-bis[4-[*N*,*N*-di(p-tolyl)amino]phenyl]cyclohexane (TCTA) and 4,4′-*N*,*N*′-dicarbazolylbiphenyl (CBP) as the host materials, respectively. The host:dopant ratios of TCTA:$Ir(ppy)_3$ and CBP:$Ir(ppy)_3$ were 97:3(v/v) and 97:4(v/v), respectively. Di-[4-(*N*,*N*-ditolyl-amino)-phenyl]cyclohexane (TAPC) (15 nm) and 1,3,5-tri(phenyl-2-benzimidazolyl)-benzene (TPBi) (65 nm) were used as hole- and electron-transporting materials, respectively. Cathode layers of lithium fluoride (LiF) (1 nm)/Al (130 nm) were deposited under high vacuum.

For fabrication of the white OLEDs, fluorescent orange-red-emitting rubrene and sky-blue-emitting DPAVBi were used as guest molecules in a fluorescent host, TBADN. To control the electron–hole balance and the recombination zone in the white OLEDs, we used a co-host composed of TBADN and NPB with a 93:7 (v/v) ratio. Other organic layers (except for the emitting layer in fluorescent white OLEDs) were deposited in the same way as for the green fluorescent OLEDs. The device structure of the white OLEDs was anode (graphene or ITO)/HIL (50 nm)/NPB (20 nm)/NPB:TBADN:rubrene (1%) (10 nm)/NPB:TBADN:DPAVBi (5%) (10 nm)/TBADN:DPAVBi (5%) (15 nm)/$Bebq_2$ (20 nm)/barium fluoride (BaF_2) (1 nm)/aluminium (130 nm), as shown in Fig. 3a. All thermal vapour depositions were carried out under high vacuum below 5×10^{-7} torr. The active area defined by the cathode was $\sim 2 \times 3$ mm^2. The devices were encapsulated with a glass lid using a UV-curable epoxy resin.

Received 11 July 2011; accepted 8 November 2011; published online 10 January 2012

References

1. Bonaccorso, F., Sun, Z., Hasan, T. & Ferrari, A. C. Graphene photonics and optoelectronics. *Nature Photon.* **4,** 611–622 (2010).
2. Rogers, J. A. Electronic materials: making graphene for macroelectronics. *Nature Nanotech.* **3,** 254–255 (2008).
3. Wu, J. *et al.* Organic light-emitting diodes on solution-processed graphene transparent electrodes. *ACS Nano* **4,** 43–48 (2010).
4. Sun, T. *et al.* Multilayered graphene used as anode of organic light emitting devices. *Appl. Phys. Lett.* **96,** 133301 (2010).
5. Novoselov, K. S. *et al.* Electric field effect in atomically thin carbon films. *Science* **306,** 666–669 (2004).
6. Geim, A. K. & Novoselov, K. S. The rise of graphene. *Nature Mater.* **6,** 183–191 (2007).
7. Zhang, Y., Tan, Y., Stormer, H. L. & Kim, P. Experimental observation of the quantum Hall effect and Berry's phase in graphene. *Nature* **438,** 201–205 (2005).
8. Kim, K. S. *et al.* Large-scale pattern growth of graphene films for stretchable transparent electrodes. *Nature* **457,** 706–710 (2009).
9. Lee, Y. *et al.* Wafer-scale synthesis and transfer of graphene films. *Nano. Lett.* **10,** 490–493 (2010).
10. Bae, S. *et al.* Roll-to-roll production of 30-inch graphene films for transparent electrodes. *Nature Nanotech.* **5,** 574–578 (2010).
11. Li, X. *et al.* Large-area synthesis of high-quality and uniform graphene films on copper foils. *Science* **324,** 1312–1314 (2009).
12. Reina, A. *et al.* Layer area, few-layer graphene films on arbitrary substrates by chemical vapor deposition. *Nano Lett.* **9,** 30–35 (2009).
13. Eda, G., Fanchini, G. & Chhowalla, M. Large-area ultrathin films of reduced graphene oxide as a transparent and flexible electronic material. *Nature Nanotech.* **3,** 270–274 (2008).
14. Matyba, P. *et al.* Graphene and mobile ions: the key to all-plastic, solution-processed light-emitting devices. *ACS Nano* **4,** 637–642 (2010).
15. Arco, L. G. D. *et al.* Continuous, highly flexible, and transparent graphene films by chemical vapor deposition for organic photovoltaics. *ACS Nano* **4,** 2865–2873 (2010).
16. Yin, Z. *et al.* Organic photovoltaic devices using highly flexible reduced graphene oxide films as transparent electrodes. *ACS Nano* **4,** 5263–5268 (2010).
17. Wu, J. *et al.* Organic solar cells with solution-processed graphene transparent electrodes. *Appl. Phys. Lett.* **92,** 263302 (2008).
18. Choe, M. *et al.* Efficient bulk-heterojunction photovoltaic cells with transparent multi-layer graphene electrodes. *Org. Electron.* **11,** 1864–1869 (2010).
19. Wang, X., Zhi, L. & Müllen, K. Transparent, conductive graphene electrodes for dye-sensitized solar cells. *Nano Lett.* **8,** 323–327 (2008).
20. Kumar, A. & Zhou, C. The race to replace tin-doped indium oxide: which material will win? *ACS Nano* **4,** 11–14 (2010).
21. Choi, M-R. *et al.* Soluble self-doped conducting polymer compositions with tunable work function as hole injection/extraction layers in organic optoelectronics. *Angew. Chem. Int. Ed.* **50,** 6274–6277 (2011).
22. Li, J. *et al.* Organic light-emitting diodes having carbon nanotube anodes. *Nano Lett.* **6,** 2472–2477 (2006).
23. Chien, Y-M., Lefevre, F., Shin, I. & Izquierdo, R. A solution processed top emission OLED with transparent carbon nanotube electrodes. *Nanotechnology* **21,** 134020 (2010).
24. Helender, M. G. *et al.* Chlorinated indium tin oxide electrodes with high work function for organic device compatibility. *Science* **332,** 944–947 (2011).
25. Poplavskyy, D., Su, W. & So, F. Bipolar charge transport, injection, and trapping studies in a model green-emitting polyfluorene copolymer. *J. Appl. Phys.* **98,** 014501 (2005).
26. Campbell, A. J., Bradley, D. D. C. & Antoniadisc, H. Quantifying the efficiency of electrodes for positive carrier injection into poly(9,9-dioctylfluorene) and representative copolymers. *J. Appl. Phys.* **89,** 3343–3351 (2001).
27. Cheung, C. H., Kwok, K. C., Tse, S. C. & So, S. K. Determination of carrier mobility in phenylamine by time-of-flight, dark-injection, and thin film transistor techniques. *J. Appl. Phys.* **103,** 093705 (2008).
28. Harding, M. J., Poplavskyy, D., Choong, V-E., So, F. & Campbell, A. J. Variations in hole injection due to fast and slow interfacial traps in polymer light-emitting diodes with interlayers. *Adv. Funct. Mater.* **20,** 119–130 (2010).
29. Jong, M. P. D., IJzendoorn, L. J. V. & Voigt, M. J. A. D. Stability of the interface between indium-tin-oxide and poly (3,4-ethylenedioxythiophene)/poly(styrenesulfonate) in polymer light-emitting diodes. *Appl. Phys. Lett.* **77,** 2255–2257 (2000).
30. Sekitani, T. *et al.* Stretchable active-matrix organic light-emitting diode display using printable elastic conductors. *Nature Mater.* **8,** 494–499 (2009).

Acknowledgements

This research was supported by the Basic Research Program and Global Frontier Research Center for Advanced Soft Electronics through the National Research Foundation of Korea (NRF), funded by the Ministry of Education, Science and Technology (nos. 2009-0067533, 2009-0075025, 2011-0006268 and 2009-0090177). This research was also supported by the Converging Research Center Program through the Ministry of Education, Science and Technology (no. 2010K001431).

Author contributions

T.-H.H. designed and conducted most of the experiments, analysed the data and prepared the manuscript. Y.L. and S.-H.B. conducted experiments regarding graphene growth, patterning of graphene anodes and characterization. S.-H.W. and M.-R.C. helped with the OLED fabrication experiments. B.H.H. interpreted data and suggested improvements to the manuscript. J.-H.A. designed the graphene experiments, analysed data and prepared the manuscript. T.-W.L. initiated the study, designed all the experiments, analysed the data and prepared the manuscript. All authors discussed the results and contributed to the paper.

Additional information

The authors declare no competing financial interests. Supplementary information accompanies this paper at www.nature.com/naturephotonics. Reprints and permission information is available online at http://www.nature.com/reprints. Correspondence and requests for materials should be addressed to J.-H.A. and T.-W.L.